*

The lysosome system is severely impaired in a cellular model of neurodegeneration induced by HSV-1 and oxidative stress

Henrike Kristen [a,b], Isabel Sastre [a,b], Teresa Muñoz-Galdeano [a,1], Maria Recuero [a,b,c], Jesus Aldudo [a,b,c,*] & Maria J. Bullido [a,b,c,*]

[a] *Centro de Biologia Molecular "Severo Ochoa" (C.S.I.C.-U.A.M.), Universidad Autonoma de Madrid, C/ Nicolas Cabrera 1, 28049 Madrid, Spain.*

[b] *Centro de Investigacion Biomedica en Red sobre Enfermedades Neurodegenerativas (CIBERNED), Madrid, Spain.*

[c] *Instituto de Investigacion Sanitaria "Hospital la Paz" (IdIPaz), Madrid, Spain.*

E-mail addresses of authors: henrike.kristen@cbm.csic.es; isastre@cbm.csic.es; tmunozd@sescam.jccm.es; mrecuero@cbm.csic.es; jaldudo@cbm.csic.es; mjbullido@cbm.csic.es;

[*] Corresponding authors:

- Jesus Aldudo, Centro de Biología Molecular "Severo Ochoa", Universidad Autónoma de Madrid, C/ Nicolás Cabrera 1, 28049 Madrid, Spain. Tel. (+34) 91-196-4674. Fax (+34) 91-196-4420. E-mail: jaldudo@cbm.csic.es

- Maria J. Bullido, Centro de Biología Molecular "Severo Ochoa", Universidad Autónoma de Madrid, C/ Nicolás Cabrera 1, 28049 Madrid, Spain. Tel. (+34) 91-196-4567. Fax (+34) 91-196-4420. E-mail: mjbullido@cbm.csic.es

[1] *Present address: Molecular Neuroprotection Laboratory, Hospital Nacional de Parapléjicos, SESCAM, Toledo, Spain*

Abbreviations: AMC: 7-Amino-4-MethylCoumarin; BCA: Bicinchoninic Acid; EBSS: Earle's Balanced Salt Solution; GWAS: Genome-Wide Association Studies; KEGG: Kyoto Encyclopedia of Genes and Genomes; LSD: Lysosomal Storage Disease; LSG: LysoSensor® Green DND-189; LTR: LysoTracker® Red DND-99; NCL: Neuronal Ceroid Lipofuscinosis; OS: Oxidative Stress; X-XOD: Xanthine and Xanthine Oxidase

Summary

The causal agent(s) and molecular mechanisms of Alzheimer's disease (AD) remain unclear. Mounting evidence suggests that HSV-1 infection is involved in the AD pathogenesis. Oxidative stress (OS) may also be crucial in the AD development. Our group previously reported that both HSV-1 and OS trigger the appearance of AD-type neurodegeneration markers. The main aim of the present study was to identify the mechanisms involved in this triggering. Expression studies revealed the involvement of a set of OS-regulated genes in HSV-1-infected cells, and in cells harboring the APP_{swe} mutation. Functional annotation of these genes revealed the lysosome system to be impaired, suggesting that the interaction of OS with both HSV-1 and APP mutations affects lysosomal function. Functional studies revealed HSV-1 infection and OS to increase the lysosome load, reduce the activity of lysosomal hydrolases, affect cathepsin maturation and inhibit the endocytosis-mediated degradation of the EGF receptor. These findings suggest alterations in the lysosome system to be involved in different forms of AD.

Keywords: HSV-1 infection; lysosome; neurodegeneration; microarrays; Alzheimer´s disease

1. Introduction

Alzheimer's disease (AD) is the most prevalent neurodegenerative disease, and is that with the highest incidence in the human population aged 65 and over. It causes progressive loss of memory and cognitive deterioration, irreversibly leading to dementia. Unfortunately, the pathogenic mechanisms involved in cognitive impairment and the eventual development of AD remain poorly understood. There is increasing evidence that chronic or latent infections of the central nervous system are involved in the neurodegenerative process, either via a direct effect of the infectious agents themselves or via the associated inflammatory response, or both (Harris and Harris, 2015; Itzhaki et al., 2016).

Numerous experimental findings suggest the implication of HSV-1 infection in AD pathogenesis (Piacentini et al., 2014). The first evidence of its involvement came from epidemiological studies showing that people who have HSV-1 DNA in the brain and who also carried the apolipoprotein E type 4 allele were at higher risk of developing AD (Itzhaki et al., 1997). Certainly, HSV-1 DNA is present in a high proportion of elderly AD brains, usually located within the amyloid plaques (Wozniak et al., 2009). Subsequent studies revealed that HSV-1 caused the accumulation of Aβ and phosphorylated tau in cell cultures (Lerchundi et al., 2011; Piacentini et al., 2015; Wozniak et al., 2007) and in mice (Martin et al., 2014; Zambrano et al., 2008), and antiviral treatment of HSV-1-infected cells greatly decreased this accumulation (Wozniak et al., 2013; Wozniak et al., 2011). Moreover, HSV infection, revealed by seropositivity, has been significantly associated with development of AD (Letenneur et al., 2008; Lovheim et al., 2015a; Lovheim et al., 2015b; Mancuso et al., 2014). Finally, the data gathered in genome-wide association studies (GWAS) involving thousands of patients with AD and controls identified a set of AD-linked gene variants that seem to

increase susceptibility to viral infection of the brain, particularly HSV-1 infection (Porcellini et al., 2010). A growing number of studies also point to oxidative stress (OS) as key in the pathogenesis of neurodegenerative diseases (Kim et al., 2015). OS has been shown to play a prominent role in the progression of AD and contribute towards the generation of Aβ deposits and neurofibrillary tangles (Cai et al., 2011). Our group has devoted several years to the development and study of neuronal models that simulate different aspects of pathogenesis, such as HSV-1 infection and OS. With this strategy, we have shown that HSV-1 is able to trigger the neurodegenerative process, inducing the appearance of the characteristic markers of AD-type neurodegeneration (Alvarez et al., 2012; Santana et al., 2012a; Santana et al., 2012b). In addition, OS has been found to strongly disturb cholesterol biosynthesis (Recuero et al., 2009) and APP metabolism/processing (Recuero et al., 2013)—processes that are altered in AD brains.

Lysosomes are the main digestive compartments within cells, and form part of two major cellular degradative pathways: autophagy and endocytosis. In recent years, substantial links between AD pathogenesis and lysosomal biology have been reported (Whyte et al., 2017). Neuron survival requires the continuous recycling of cellular materials released by the machineries of autophagy and endocytosis, but neurons are particularly vulnerable to disruption of the lysosome system. Indeed, the lysosomal storage diseases (LSDs)—a group of some 50 metabolic disorders that arise from inherited mutations causing the deficiency of a protein required for proper lysosomal function (Filocamo and Morrone, 2011), and which are associated with the accumulation of lysosomes and autophagic vesicles—cause severe neurodegenerative phenotypes. In fact, given the extensive autophagic-endocytic-lysosomal neuropathology seen in the early stages of certain neurodegenerative processes, some authors postulate that these, and particularly AD, should be included among the LSDs

(Nixon et al., 2008; Wolfe et al., 2013). The enlargement of endosomal compartments, perturbed trafficking of lysosomal enzymes, progressive accumulation of autophagic vesicles and deficits of lysosomal function are all well-recognized as early neuropathological markers of sporadic AD (Neefjes and van der Kant, 2014; Peric and Annaert, 2015). Together, these findings support the idea that alterations in lysosomal function might contribute significantly to the neurodegeneration associated with AD.

Our group has reported risk polymorphisms in candidate genes related to HSV-1 infection (Bullido et al., 2007; Bullido et al., 2008) and the response to OS (Recuero et al., 2009), supporting the idea that the latter challenges contribute towards the pathogenesis of AD. We have also reported HSV-1 infection and OS to interact and promote the appearance of AD-like neurodegeneration events in neuronal cell models (Santana et al., 2013). The aim of present work was to determine, via differential gene expression in whole genome microarrays, which genes/pathways are important in the neurodegeneration induced by HSV-1 and OS. Functional genomic analysis of these models revealed the lysosome system to be the main system altered, while functional studies indicated HSV-1 and OS to severely affect the lysosome load and lysosomal activity. These findings suggest that lysosomal dysfunction plays an important role in the AD-like phenotype induced by HSV-1 and OS in neuronal cell models and perhaps in clinical AD.

2. Materials and Methods

2.1. Drugs and antibodies

Epidermal growth factor (EGF) was purchased from Calbiochem, xanthine and bafilomycin A1 were purchased from Sigma. Xanthine oxidase and leupeptin were

obtained from Roche and 4', 6-diamidino-2-phenylindole (DAPI) and ammonium chloride from Merck. The antibodies used in this work were: rabbit anti-EGF receptor (EGFR) (1005) (Santa Cruz Biotech; sc-03), anti-human CD63, anti-LAMP1 and anti-human LAMP2 (Developmental Studies Hybridoma Bank, University of Iowa; H5C6, H4A3 and H4B4, respectively), rabbit anti-cathepsin B (FL-339) (Santa Cruz Biotech; sc-13985), mouse monoclonal anti-human CD222 (Bio-Legend, clone MEM-238; 315902), mouse anti-early endosome antigen 1 (EEA1) (BD Biosciences; 610457), and mouse monoclonal anti-tubulin (Sigma; clone B-5-1-2; T5168). The secondary antibodies used for immunostaining were horseradish peroxidase-coupled anti-mouse (Vector; PI-2000) and anti-rabbit (Nordic; GAR/IgG(H+L)/PO) antibodies, and antibodies labeled with Alexa Fluor 488 (Thermo Fisher; A-21206) or 555 (Thermo Fisher; A-31570).

2.2. Cell culture

All cell lines used in this work were purchased from the American Type Culture Collection. SK-N-MC human neuroblastoma cells were grown as monolayers in minimal Eagle's medium (MEM) supplemented with 10% heat-inactivated fetal bovine serum (FBS; Gibco; 10270-106), 2 mM glutamine and 50 mg/ml gentamicin. SK-N-MC cells stably transfected with human wild-type APP695 (SK-APP_{wt}) or mutant APP695 harboring the Swedish mutation (K670N/M671L) (SK-APP_{swe}) were prepared in-house and commercialized by NeuronBio. Vero and HeLa cells were passaged in Dulbecco's modified Eagle's medium (DMEM) supplemented with 10% FBS, 2 mM glutamine and 50 mg/ml gentamicin. All cells were grown at 37ºC in a 5% CO_2 atmosphere.

2.3. Infection conditions and exposure to oxidative stress

The wild-type HSV-1 strain KOS 1.1 was propagated and purified from Vero cells as previously described (Burgos et al., 2002). SK-N-MC cells seeded in complete MEM at 70–80% confluency were exposed to HSV-1 at 37ºC for 1 h. Mock infections were performed using a virus-free suspension. Unbound virus was removed and the cells incubated in complete MEM at 37ºC. Time and multiplicity of infection (moi; expressed as plaque-forming units [pfu] per cell) are indicated in each experiment. The infectious titers of HSV-1 were determined by plaque assay as previously described (Santana et al., 2013). OS was induced through the addition of xanthine (10 μM) and xanthine oxidase (50 mU/ml) (X-XOD) to fresh medium. Exposure times are indicated in each experiment. In samples exposed to OS and HSV-1, X-XOD was added after the adsorption of the virus and maintained until the end of infection.

2.4. EGF receptor degradation assay

HeLa cells were cultured in serum-free medium for at least 6 h before the treatments with HSV-1 and X-XOD. After HSV-1 adsorption/X-XOD addition, cells were incubated with medium containing 2% FBS. To stimulate EGF receptor endocytosis, EGF (40 ng/ml) was added at the times indicated in each experiment. Cells were collected at various time points and analyzed by Western blotting or immunofluorescence. For immunoblotting, cells were lysed in RIPA buffer (50 mM Tris-HCl pH 7.5, 1% Triton X-100, 150 mM NaCl, 1 mM EDTA and 0.1% sodium deoxycholate) containing a protease inhibitor cocktail (Roche) and incubated for 30 min at 4ºC. Lysates were centrifuged at 13,000 *g* for 15 min at 4ºC. The protein concentration of the lysates was quantified using the BCA protein assay (Pierce). Cell lysates were mixed with 2× Laemmli buffer, heated for 5 min at 100ºC, and then subjected to SDS-PAGE and immunoblotted using an anti-EGFR and an anti-tubulin antibody to ensure equal loading. The secondary antibody was conjugated with

horseradish-peroxidase and detection performed using the Amersham ECL Western Blotting Detection Reagent (GE Healthcare). For immunofluorescence, cells were cultured on coverslips, fixed with 4% formaldehyde for 10 min, and incubated with an anti-EGFR antibody in combination with either anti-EEA1, anti-CD222 or anti-CD63 followed by incubation with appropriate Alexa-Fluor-coupled secondary antibodies. Cells were counterstained with DAPI to visualize the nuclei. All cells were examined using a Zeiss LSM710 confocal microscope equipped with an oil-immersion objective running ZEN2010 software (Carl Zeiss Microscopy GmbH). Images were processed using Adobe Photoshop CS4.

2.5. Colocalization analysis

Colocalization analysis of confocal images stained with EGFR and endolysosomal markers (EEA1, CD222 and CD63) was performed with the Image-J 1.51u software. Each image was split into red and green channels, and analyzed on an identical-sized region of interest (ROI) selected for each channel. A total of 25 cells were analyzed. Colocalization was quantified using Pearsons´s correlation coefficients determined with the Just another Colocalization Plugin (JaCoP) plugin (Bolte and Cordelieres, 2006).

2.6. Quantification of lysosome load

The lysosome load was determined using the acidotropic probes LysoSensor® Green DND-189 (LSG) and LysoTracker® Red DND-99 (LTR) (both from Molecular Probes). These probes pass freely through cell membranes and typically concentrate in acidic organelles. As a control, cells were exposed to ammonium chloride (20 mM) and nutrient starvation; for this, the culture medium was exchanged for Earle's balanced salt solution (EBSS). One hour before the end of treatments, cells were exposed to 0.1 μM LSG or 1 μM LTR for 1 h at 37°C in culture medium and then washed with PBS. For

LTR, cells were lysed with RIPA buffer for 30 min at 4ºC and the lysates centrifuged at 13,000 *g* for 10 min. The protein concentration of the lysates was quantified by the BCA method, and fluorescence recorded using a FLUOstar OPTIMA microplate reader (BMG LABTECH) (excitation wavelength 560 nm, emission wavelength 590 nm). Alternatively, cells were fixed with 2% formaldehyde and the LSG fluorescence emitted by 10,000 cells in the FL-1 channel (530/30 nm) quantified using a FACSCalibur flow cytometer (BD Biosciences) running with CellQuest Pro software. Data analysis was performed using Flow Jo software.

2.7. Cathepsin activity assays and maturation analysis

The enzymatic activity of different cathepsins was determined as previously described with minor modifications (Porter et al., 2013). Briefly, SK-N-MC cells were lysed for 30 min at 4°C with shaking in 50 mM sodium acetate (pH 5.5), 0.1 M NaCl, 1 mM EDTA, and 0.2% Triton X-100. Lysates were clarified by centrifugation and immediately used for determination of proteolytic activity. 25-75 µg of protein from cell lysates were incubated for 30 min in the presence of the following fluorogenic substrates (all from Enzo Life Sciences): Z-VVR-AMC (P-199; most sensitive substrate for cathepsin S; 20 µM), Z-GPR-AMC (P-142; specific for cathepsin K; 20 µM), Z-RR-AMC (P-137; specific for cathepsin B; 20 µM) and the Cathepsin D/E fluorogenic substrate Mca-GKPILFFRLK(Dnp)-D-Arg-NH_2 (P-145; 10 µM). The AMC released was quantified with a microtiter plate reader (Tecan Trading AG) with excitation at 360 nm and emission at 430 nm (Z-VVR-AMC, Z-GPR-AMC and Z-RR-AMC), or 320 nm and 400 nm (Cathepsin D and E fluorogenic substrate). To analyze the maturation of cathepsin B, SK-N-MC cell lysates were obtained as above, except that a protease inhibitor cocktail (Roche) was added to the lysis buffer. As a control, cells were exposed to ammonium chloride (20 mM) and bafilomycin A1 (100 nM) to induce

lysosomal inhibition. Cell lysates were mixed with 2× Laemmli buffer, heated for 5 min at 100ºC, and then subjected to SDS-PAGE and immunoblotted using an anti-cathepsin B and an anti-tubulin antibody to ensure equal loading.

2.8. Microarray assay, data pre-processing and data analysis

Total RNA was obtained from untreated and X-XOD-treated cells (three independent culture replicates for each condition) using the High Pure RNA Isolation Kit (Roche). The integrity and quantity were checked using an Agilent Bioanalyzer. The One-Color Microarray-Based Gene Expression Analysis Protocol (Agilent Technologies) was used to amplify and label RNA. Samples were hybridized on whole human genome microarrays 4×44 k (Agilent Technologies). 1.65 µg of Cy3-labeled RNA were hybridized for 17 h at 65°C in a hybridization oven (Agilent Technologies) set at 10 rpm, in a final concentration of 1× GEx Hybridization Buffer HI-RPM (Agilent Technologies). The arrays were then washed and dried using a centrifuge according to the manufacturer's instructions, and scanned at 5 mm resolution in a DNA Microarray Scanner (Agilent Technologies) using the default settings for 4×44 k format one-color arrays. Images provided by the scanner were analyzed using Feature Extraction software v.10.7.3.1 (Agilent Technologies). Raw signals were threshold to 1 and quantile normalization (Bolstad et al., 2003) performed using GeneSpring software. Data were expressed on a log2 scale. Of the 41,105 probes present in the chip, those fulfilling the following criteria were deemed suitable for further analysis: (i) promoting a signal within the higher 80th percentiles in at least 75% of the replicates in one condition; (ii) flagging at least 75% of the replicates in a given condition as present or marginal, and (iii) showing a coefficient of variation across samples of > 2.5%. Quality control checks were based on the bioconductor package ArrayQualityMetrics

(www.bioconductor.org). All samples employed for analysis were processed using the Limma bioconductor package (Smyth, 2004). For each comparison, genes with a Benjamini-Hochberg corrected p-value < 0.05 were considered differentially expressed (Benjamini and Hochberg, 1995). Unless otherwise stated, each comparison focused on the genes differentially expressed and with a change of at least 1.2-fold between the compared conditions. Genes that were differentially expressed were uploaded to bioinformatic tools for data mining. Gene annotation co-occurrence discovery (GeneCodis; genecodis.cnb.csic.es) and ingenuity pathway analysis (Ingenuity® Systems, www.ingenuity.com) were used to identify pathways and functions significantly over- or underrepresented in the gene lists compared to the whole human genome.

2.9. Quantitative RT-PCR

The mRNA transcribed from each gene was quantified by two-step reverse transcription PCR ([RT]-PCR) using TaqMan low density arrays (Applied Biosystems) as previously described (Recuero et al., 2009). Briefly, total RNA isolated from SK-N-MC cells was subjected to reverse transcription using the High Capacity cDNA Archive Kit (Applied Biosystems). Real-time PCR was then performed in an ABI Prism 7900HT SD® (Applied Biosystems) using TaqMan arrays for the following genes: *GAPDH* - Hs02758991_g1; *ATP6AP1*: Hs00184593_m1; *ATP6V1H*: Hs00977530_m1; *CTSB*: Hs00947433_m1; *CTSF* - Hs00186901_m1; *LAMP2* - Hs00174474_m1; *LIPA* - Hs01548815_m1; *NPC1* - Hs00264835_m1; and *NPC2* - Hs00197565_m1. The relative quantities in treated and untreated cells were determined by the ΔΔCt method using SDS v.2.1.1 software. *GAPDH* was used as the housekeeping gene, the expression of which did not change at any time.

2.10. Data analysis

Data are shown as means ± standard error of the mean (SEM). Differences between groups were analyzed pairwise using the 2-tailed Student t test. Significance was recorded at $p<0.05$ (*), $p<0.01$(**), and $p<0.001$(***). Before analysis, the largest and the smallest variances were tested for homogeneity using the F-test.

3. Results

3.1. Microarray gene expression studies revealed alterations in the lysosome system

To study the impact of HSV-1 infection and OS on gene expression, and to identify putative genes and/or pathways associated with AD, a microarray analysis covering the whole human genome was performed for SK-N-MC human neuroblastoma cells. To mimic the situation of endogenous infection in AD brains, a cell model of HSV-1 infection at a low viral dose in the presence of mild OS for 24 and 36 h was established. In earlier work, we developed a neuronal cell model of mild oxidative stress using the free radical generating system xanthine/xanthine oxidase (X-XOD). This cell model allowed the analysis of free radical-induced events preceding cell death. X-XOD induced an increase in the production of radical oxygen species (Recuero et al., 2010) and in cytosolic calcium levels, finally leading to apoptotic cell death (Recuero et al., 2009). A cellular model for familial AD (SK-APP_{swe}) was also exposed to OS for 24 and 36 h. Compared to the respective controls (non-infected SK-N-MC cells and SK-APP_{wt} cells), a full 833 genes were modulated by OS in the infection cell model, and 158 genes in the familial AD cell model at 24 h of treatment (Supplementary Figure 1). To identify common pathogenic mechanisms for sporadic and familial AD, the focus

was set on those genes regulated by OS in both models. This identified 65 genes significantly overexpressed (fold change > 1.2) and three significantly repressed (fold change < 0.8) for a p-value cut-off of 0.05. The complete list of genes is shown in Supplementary Table 1. To study the pathways associated with differently expressed genes, Gene Annotation Co-occurrence Discovery (GeneCodis) software was used (Carmona-Saez et al., 2007; Nogales-Cadenas et al., 2009; Tabas-Madrid et al., 2012). As shown in Table 1, significant enrichment was noted for the Kyoto Encyclopedia of Genes and Genomes (KEGG) pathway 04142: "Lysosome". Five genes of the above 68—cathepsin F (*CTSF*), lipase A, lysosomal acid, cholesterol esterase (*LIPA*); ATPase, H^+ transporting, lysosomal accessory protein 1 (*ATP6AP1*); Niemann-Pick disease, type C1 (*NPC1*); and lysosomal-associated membrane protein 2 (*LAMP2*)—were annotated to the lysosome system in which they have different roles. To confirm the GeneCodis results, the same gene list was examined using the Ingenuity Pathway Analysis software's core analysis routine (Ingenuity® Systems, www.ingenuity.com). The top annotated Diseases & Functions category was "lysosomal storage disease" with a p-value of 1.42×10^{-5}. These results identify the lysosome pathway as the main function altered.

Quantitative RT-PCR was used to verify the expression of eight selected lysosomal genes, including the five genes annotated to the lysosome system in the cell models. Supplementary Figure 2 shows the expression values obtained at 24 and 36 h when modulated by HSV-1 or OS alone, or in combination. All the genes except for *CTSB* were upregulated by X-XOD treatment at 24 h in infected and non-infected cells, suggesting that the lysosome system was regulated by OS. Gene expression continued to increase at 36 h in non-infected cells. This increase did not appear in infected cells suggesting that HSV-1 and OS interact in the regulation of this system. These genes

were also overexpressed in the familial cell model in the presence of X-XOD (unpublished observations). These results led to the undertaking of a functional analysis of this system in the HSV-1 infection model.

3.2. HSV-1 and OS enhance the lysosome load

The gene expression microarray data for the OS-treated HSV-1-infected and familial AD cellular models revealed the significant upregulation of genes related to the lysosome system. The impact of HSV-1 and OS on the lysosome system was therefore studied with the aim of investigating the possible alterations induced by these factors. Previous work by our group has shown that the greatest effect on neurodegenerative events provoked by HSV-1 and OS is achieved with a moi of 10 pfu/cell at 18 h. These conditions ensure that almost all cells are infected, and were therefore used in the following experiments.

The effect of HSV-1 and OS on the quantity of lysosomes was first explored. The total lysosome load was monitored by using two lysosomotropic probes: LysoSensor Green (LSG) and LysoTracker Red (LTR). The intensity of fluorescence of LSG is pH-dependent and is commonly used to examine lysosomal pH changes. When the effects of HSV-1 and OS were examined by FACS analysis, a significant increase in LSG staining was observed in the infected cells, independent of their oxidative status (Figure 1A). To confirm the effect of the treatments on the lysosomal compartment, LTR fluorescence was recorded; LTR concentrates in acidic organelles but, unlike LSG, its fluorescence intensity is not dependent on pH. Quantification of the LTR fluorescence levels confirmed the significant increase in the lysosomal content provoked by HSV-1. In this case, OS also caused LTR fluorescence to increase. No synergistic effect was seen between HSV-1 infection and OS (Figure 1B). These fluorescence assays were

validated using two modulators of lysosomal activity: ammonium chloride (a lysosomotropic agent that neutralizes lysosomal pH) and nutrient starvation (a positive control to increase lysosomal content) (Figure 1C). The elevation of the fluorescence intensity of the lysosomotropic probes induced by HSV-1 and OS indicates an increase in the lysosome load. This increase was also evaluated by monitoring the amount of the two most abundant proteins in lysosomes—LAMP1 and LAMP2. Both proteins were enriched in cells exposed to HSV-1 and X-XOD (Figure 1D), confirming the accumulation of lysosomes observed in the experiments with lysosomotropic probes.

3.3. Lysosomal function is impaired by HSV-1 and OS

Since cells exposed to HSV-1 and OS showed an increase in their lysosome loads, perturbations in lysosomal function and endocytic trafficking were sought by assessing the activity and maturation of lysosomal cathepsins and the degradation of EGFR.

3.3.1. HSV-1 and OS inhibit the activity of lysosomal cathepsins

The role of HSV-1 infection and OS on lysosomal proteolysis was examined by monitoring the enzymatic activity of several lysosomal cathepsins, employing fluorogenic substrates specific for cathepsins B (Figure 2A), D/E (Figure 2B), K (Figure 2C) and S (Figure 2D). All cathepsin activities recorded in SK-N-MC cells grown under OS were significantly lower than in control cultures. Similar (though less outstanding) results were seen for HSV-1-infected cells, suggesting that both factors trigger a defect in the proteolytic activity of lysosomes. No synergistic effect was observed between HSV-1 infection and OS.

Among the lysosomal proteases, cathepsin B has a broad specificity and plays a major role in intracellular protein degradation. Cathepsin B is activated by proteolysis in the acidified lysosome to produce a mature proteolytic product (Turk et al., 2001). To

assess the impact of HSV-1 infection and OS on activation state of this cathepsin, immunoblot analysis of cell lysates that have been stabilized by the addition of lysosomal inhibitors were performed (Figure 2E). HSV-1 did not affect the mature cathepsin B levels, indicating that reduced cathepsin B activity was not due to defects in its processing. However, OS induced a significant decrease in the amount of mature cathepsin B and a concomitant increase of the procathepsin B levels. Bafilomycin A1 and ammonium chloride, two agents that neutralize the pH of lysosomes, also blocked the maturation of cathepsin B, suggesting that OS could be affecting the lysosome pH. In fact, OS is known to cause permeabilization of the lysosomal membrane, thereby causing lysosome alkalization (Johansson et al., 2010). These data indicate a different nature of lysosomal dysfunction in cells infected with HSV-1 and exposed to OS.

To confirm that the impairment of the lysosome system also takes place in cells treated in the same way as in the microarray experiments, the quantity and functionality of lysosomes were determined. Both at 24 and 36 h, cells exposed to HSV-1 and OS (both separately and in combination) showed a marked increase in their lysosomal content (revealed via increased LTR fluorescence) (Figure 3A) and significantly reduced cathepsin B and D/E activity (Figure 3B).

Taken together, these results confirm that lysosome load and proteolysis are severely compromised by HSV-1 infection and OS.

3.3.2. Lysosomal degradation of EGFR is affected by HSV-1 and OS

A standard test for assessing receptor-mediated lysosomal degradation is to monitor EGFR levels. Upon EGF stimulation, EGFR is internalized by clathrin-mediated endocytosis and efficiently degraded by the lysosome system. These experiments were performed in HeLa cells since SK-N-MC cells do not express endogenous EGFR (van

Weering et al., 1995). Previous studies have shown that the stimulation of HeLa cells with EGF can result in up to 80% EGFR degradation (Laketa et al., 2014). These data are consistent with those obtained by our group showing a 75% EGFR degradation after 3 h of EGF treatment (Figure 4A). When the impact of HSV-1 and OS on EGFR degradation was studied by Western blot analysis, total EGFR levels remained higher in HeLa cells exposed to HSV-1 and OS compared to untreated cells (Figure 4A). These results were confirmed by immunofluorescence experiments. In untreated cells, EGFR was mainly localized to the plasma membrane and, after the addition of EGF, was internalized and rapidly degraded. In contrast, HSV-1 and OS induced a strong increase in EGFR intracellular staining (Figure 4B), suggesting both treatments led to a defect in EGF-induced EGFR degradation.

Since EGFR is internalized by the endocytic machinery and then degraded by the lysosomes, tests were made to determine whether EGFR accumulation induced by HSV-1 and OS takes place in some compartment of this pathway. The distribution of EGFR was examined by confocal microscopy analysis using antibodies specific to marker proteins of early endosomes (EEA1), late endosomes (insulin-like growth factor 2 receptor, CD222) and lysosomes (CD63, a lysosomal membrane protein) (Figure 5A). Endogenous EGFR was undetectable in untreated cells after 5 hours of EGF stimulation (Figure 4B). No significant colocalization of EGFR with early endosomal or lysosomal markers was detected in HSV-1-infected cells. However, confocal images revealed EGFR to colocalize significantly with CD222 in HSV-1-infected cells independently of their oxidative status, indicating an impairment of EGFR trafficking that causes the accumulation of EGFR in late endosomes. In contrast, OS induced an increase in the colocalization of EGFR and CD63 staining, showing that EGFR is able to reach the lysosome in this condition (Figure 5B).

To exclude that low levels of colocalization of EGFR and CD63 could result from rapid lysosomal degradation of EGFR in infected cells, the confocal analysis was repeated in the presence of the lysosomal inhibitors leupeptin and ammonium chloride (Figure 6A). In these conditions, no colocalization of CD63 with EGFR was detected, confirming the impairment of the transport of EGFR to the lysosomes in cells exposed to HSV-1. In contrast, inhibition of lysosomal function caused a huge increase of the lysosomal localization of EGFR in untreated cells, and a small but significant increase of the lysosomal localization of EGFR in X-XOD-treated cells (Figure 6B). Similar results were obtained with the lysosomal inhibitor bafilomycin A1 (unpublished observations). These results suggest that only some of the EGFR molecules are degraded by lysosomes in cells exposed to OS indicating a defect in the lysosomal degradation.

4. Discussion

The present results show that HSV-1 infection and OS can induce significant defects in the functioning of the lysosome system. These findings are supported by those of several GWAS that identify polymorphisms associated with AD to affect endocytosis and lipid metabolism (Harold et al., 2009; Jones et al., 2010; Lambert et al., 2009; Lambert et al., 2013). How the latter contribute to neurodegeneration is under intense investigation, but it is already known that some of these variations result in abnormal trafficking in the endo-lysosomal and autophagic networks (Cormont et al., 2003; Moreau et al., 2014). Interestingly, several of these variations—namely *APOE*, *ABCA7*, *CD2AP*, and *PICALM*—have been directly or indirectly associated with the herpes simplex life cycle, supporting the involvement of HSV-1 in AD pathogenesis (Licastro et al., 2011; Porcellini et al., 2010). The latter authors suggest that these genes

(among others) give rise to a genetic signature that might affect the ability of the central nervous system to fight herpesvirus infection. These findings agree with the present results and together they suggest the lysosome system to be important in AD pathogenesis and strengthen the hypothesis that HSV-1 has a causal role in AD.

Experiments with the lysosomotropic probes LTR and LSG showed the significant increase in the lysosome load caused by HSV-1 infection and OS. However, while the lysosome load also increased under OS, only the LTR fluorescence increased. Unlike LTR, LSG fluorescence is pH-sensitive and may indicate changes in lysosomal mass or pH. OS is known to cause the permeabilization of the lysosomal membrane, thereby releasing hydrolases from the lysosomal lumen into the cytosol and causing lysosome alkalization (Johansson et al., 2010). In this context, a recent report showed that sub-lethal OS induces lysosome biogenesis and lysosomal membrane permeabilization in rat myoblasts (Leow et al., 2017). Interestingly, increased concentrations of lysosomal proteins have been found in the cerebrospinal fluid and brains of patients with AD (Armstrong et al., 2014; Barrachina et al., 2006), and the accumulation of lysosomes is a well-known hallmark of AD brains (Cataldo et al., 1995; Cataldo et al., 1996; Gowrishankar et al., 2015). The increase in the lysosome load induced by HSV-1 and OS is consistent with the overexpression of lysosomal genes and the enhanced amount of the two most abundant lysosomal proteins—LAMP1 and LAMP2—observed in our cell model of infection and OS. A number of studies have shown that upregulation of lysosomal proteins might be involved in protecting neurons against toxicity and damage (Bendiske and Bahr, 2003; Hawkes et al., 2006).

Given the increased lysosome load caused by HSV-1 and OS, the effect of both stimuli on lysosomal proteolytic activity was examined. Cathepsins are abundant lysosomal endopeptidases that catalyze the hydrolysis of a wide variety of substrates.

HSV-1 infection and OS significantly reduced the activity of cathepsins B, K, S, and D/E. Numerous examples of the inhibition of lysosomal enzymatic activity by OS have been reported (Porter et al., 2013). Importantly, mutations in *CTSD* cause neuronal ceroid lipofuscinosis (NCL) (a human LSD associated with severe mental retardation and dementia), and *CTSF* and *D* removal in mice lead to a phenotype that resembles NCL (Koike et al., 2000; Tang et al., 2006). In addition, inhibition and/or loss of cathepsin B and L lead to lysosomal dysfunction and the accumulation of intracellular cholesterol and Aβ (Cermak et al., 2016). Finally, there are several reports of reduced lysosomal enzyme activity in association with AD (recently reviewed in (Whyte et al., 2017). These studies indicate the importance of cathepsin activity in maintaining lysosomal function and preventing neurodegenerative processes. In conclusion, HSV-1 and OS appear to induce an increase in the lysosome load that does not correlate with any increase in lysosomal enzyme activity. Further, HSV-1 and OS severely impair the proteolytic activity of lysosomes. All these findings suggest that the lysosomal defects reported in our cell model of infection and OS are not directly related to the alteration of lysosomal gene expression. Rather, the upregulation of lysosomal genes could represent a protective cell response to increase lysosome biogenesis and therefore enhance the degradative capacity of lysosomes.

The impairment of the endocytic pathway is one of the earliest events in AD (Peric and Annaert, 2015). Defects in it have been associated with lysosomal dysfunction, and were evaluated in the present cell model. The results revealed the accumulation of EGFR in late endosomes in HSV-1-infected cells, indicating endosomal trafficking to have been affected by infection. In line with these findings, no significant colocalization of EGFR and the lysosomal protein CD63 was observed in cells exposed to HSV-1 in the presence of lysosomal inhibitors indicating that EGFR is

unable to reach the lysosome. This endosomal accumulation suggests that the final step of this pathway—the fusion of late endosomes with lysosomes—is altered by the virus. Along these lines, HSV-1 glycoprotein B has been reported to impair endosomal trafficking (Niazy et al., 2017), and we previously described that the fusion of lysosomes with autophagosomes was also strongly altered in HSV-1-infected cells (Santana et al., 2012a). Thus, neither during endocytosis nor autophagy (which converge in the lysosome) can vesicular cargoes be delivered to the lysosomes, causing an accumulation of autophagosomes and late endosomes in infected cells. In contrast, colocalization of EGFR with lysosomal markers was significantly increased in cells exposed to OS, both in the absence and in the presence of lysosomal inhibitors. Thus, EGFR is able to reach the lysosome but its degradation is inefficient in cells exposed to OS. These results indicate a different nature of lysosomal dysfunction between HSV-1 and OS conditions. In addition, there are also differences between HSV-1-infected cells and cells exposed to OS when analyzing the maturation process of cathepsins. Similar to other proteases, cathepsins are synthesized as inactive precursors and, in the acidic environment of the lysosome, are activated by proteolytic removal of the N-terminal propeptide (Turk et al., 2001). OS strongly blocked the maturation of cathepsin B suggesting that lysosome pH could be altered, whereas HSV-1 did not affect the maturation process. All of these data suggest that OS cause lysosome alkalization. Since lysosomal proteases are optimally active at low pH, the increase in lysosomal pH could explain the lysosomal localization of EGFR, the overall decrease in cathepsin activities, and the inhibition of the maturation of cathepsin B induced by OS. Additional studies are needed to determine the molecular mechanisms behind the lysosomal degradation failure occurring in infected cells.

Taken together, the present results strongly suggest the involvement of the lysosome system in the AD-like phenotype induced by HSV-1 and OS in neuronal cell models. Numerous studies support the role of lysosomal dysfunction in neurodegeneration, and the enhancement of lysosome efficiency in patients with AD might be a therapeutic strategy worth exploring. The stimulation of transcription factor EB (TFEB) function—the master regulator of lysosomal biogenesis—has recently been suggested to be neuroprotective in different mouse models of neurodegenerative diseases (Polito et al., 2014; Xiao et al., 2015). In addition, the genetic deletion of cystatins (endogenous inhibitors of cysteine proteases, including several cathepsins) has been reported to attenuate amyloidogenesis and improve synaptic and cognitive function in AD mouse models (Sun et al., 2008; Yang et al., 2014).

In summary, HSV-1 and OS increased the lysosome load, reduced the activity of different lysosomal hydrolases, and led to defective endocytosis-mediated EGFR degradation in a cellular model of AD, suggesting the lysosome system to have been impaired. Functional genomic analysis suggested the same. These alterations might contribute to neurodegeneration by reducing the degradation of toxic aggregates. Lysosomal dysfunction may therefore play a major role in the onset of AD, and deserves further exploration.

ACKNOWLEDGEMENTS

We thank Susana Molina for helping in the APP stable cell lines generation. Henrike Kristen is recipient of a UAM-CSIC International Excellence Campus research contract. Institutional grants from the *Fundación Ramón Areces* and *Banco de Santander* to the *CBMSO* are also acknowledged. This work was supported by the Spanish *Ministerio de*

Ciencia e Innovación (SAF2014-53954-R). The funding source had no role in study design, collection, analysis and interpretation of data, in writing of the report or the decision to submit for publication.

Table 1. Functional annotation of the genes regulated by oxidative stress in cells infected with HSV-1 or carrying the APPswe mutation

Item Code	Item Name	NG	Hyp*	Genes
Kegg:04142	Lysosome	5	6.58E-05	CTSF, NPC1, LIPA, LAMP2, ATP6AP1
GO:0002576	platelet degranulation	3	0.0045	VEGFB, STXBP1, LAMP2
GO:0007596, GO:0030168	blood coagulation, platelet activation	4	0.0050	VEGFB, PDE1A, LAMP2, SLC8A2
GO:0006629	lipid metabolic process	4	0.0055	FADS2, LIPA, ACSL4, LIPH
GO:0007596	blood coagulation	5	0.0066	VEGFB, MAFF, PDE1A, LAMP2, SLC8A2
GO:0006811	ion transport	5	0.0092	SLC22A18, SCN4B, KCNAB2, ATP6AP1, SLC8A2
GO:0001525	angiogenesis	3	0.0097	ANG, MFGE8, FZD5
GO:0008152	metabolic process	4	0.0098	ANG, UGT3A2, METTL7A, FAP

The input list (the 68 genes of interest) was compared with the annotated human genome (34208 items) to identify KEGG Pathways, Gene Ontology Cellular Functions or Gene Ontology Molecular Functions over or underrepresented, using the GeneCodis annotation tool (http://genecodis.cnb.csic.es). The resultant items with a corrected p value<0.01 and the symbol of the annotated genes are shown. NG = Number of annotated genes in the input list; Hyp* = Corrected hypergeometric p value.

Alvarez, G., Aldudo, J., Alonso, M., Santana, S., Valdivieso, F., 2012. Herpes simplex virus type 1 induces nuclear accumulation of hyperphosphorylated tau in neuronal cells. J Neurosci Res 90(5), 1020-1029.
Armstrong, A., Mattsson, N., Appelqvist, H., Janefjord, C., Sandin, L., Agholme, L., Olsson, B., Svensson, S., Blennow, K., Zetterberg, H., Kagedal, K., 2014. Lysosomal network proteins as potential novel CSF biomarkers for Alzheimer's disease. Neuromolecular Med 16(1), 150-160.
Barrachina, M., Maes, T., Buesa, C., Ferrer, I., 2006. Lysosome-associated membrane protein 1 (LAMP-1) in Alzheimer's disease. Neuropathol Appl Neurobiol 32(5), 505-516.
Bendiske, J., Bahr, B.A., 2003. Lysosomal activation is a compensatory response against protein accumulation and associated synaptopathogenesis--an approach for slowing Alzheimer disease? J Neuropathol Exp Neurol 62(5), 451-463.
Benjamini, Y., Hochberg, Y., 1995. Controlling the False Discovery Rate: A Practical and Powerful Approach to Multiple Testing. Journal of the Royal Statistical Society. Series B (Methodological) 57(1), 289-300.
Bolstad, B.M., Irizarry, R.A., Astrand, M., Speed, T.P., 2003. A comparison of normalization methods for high density oligonucleotide array data based on variance and bias. Bioinformatics 19(2), 185-193.
Bolte, S., Cordelieres, F.P., 2006. A guided tour into subcellular colocalization analysis in light microscopy. J Microsc 224(Pt 3), 213-232.
Bullido, M.J., Martinez-Garcia, A., Artiga, M.J., Aldudo, J., Sastre, I., Gil, P., Coria, F., Munoz, D.G., Hachinski, V., Frank, A., Valdivieso, F., 2007. A TAP2 genotype associated with Alzheimer's disease in APOE4 carriers. Neurobiol Aging 28(4), 519-523.
Bullido, M.J., Martinez-Garcia, A., Tenorio, R., Sastre, I., Munoz, D.G., Frank, A., Valdivieso, F., 2008. Double stranded RNA activated EIF2 alpha kinase (EIF2AK2; PKR) is associated with Alzheimer's disease. Neurobiol Aging 29(8), 1160-1166.
Burgos, J.S., Ramirez, C., Sastre, I., Bullido, M.J., Valdivieso, F., 2002. Involvement of apolipoprotein E in the hematogenous route of herpes simplex virus type 1 to the central nervous system. J Virol 76(23), 12394-12398.
Cai, Z., Zhao, B., Ratka, A., 2011. Oxidative stress and beta-amyloid protein in Alzheimer's disease. Neuromolecular Med 13(4), 223-250.
Carmona-Saez, P., Chagoyen, M., Tirado, F., Carazo, J.M., Pascual-Montano, A., 2007. GENECODIS: a web-based tool for finding significant concurrent annotations in gene lists. Genome Biol 8(1), R3.
Cataldo, A.M., Barnett, J.L., Berman, S.A., Li, J., Quarless, S., Bursztajn, S., Lippa, C., Nixon, R.A., 1995. Gene expression and cellular content of cathepsin D in Alzheimer's disease brain: evidence for early up-regulation of the endosomal-lysosomal system. Neuron 14(3), 671-680.
Cataldo, A.M., Hamilton, D.J., Barnett, J.L., Paskevich, P.A., Nixon, R.A., 1996. Properties of the endosomal-lysosomal system in the human central nervous system: disturbances mark most neurons in populations at risk to degenerate in Alzheimer's disease. J Neurosci 16(1), 186-199.
Cermak, S., Kosicek, M., Mladenovic-Djordjevic, A., Smiljanic, K., Kanazir, S., Hecimovic, S., 2016. Loss of Cathepsin B and L Leads to Lysosomal Dysfunction, NPC-Like Cholesterol Sequestration and Accumulation of the Key Alzheimer's Proteins. PLoS One 11(11), e0167428.
Cormont, M., Meton, I., Mari, M., Monzo, P., Keslair, F., Gaskin, C., McGraw, T.E., Le Marchand-Brustel, Y., 2003. CD2AP/CMS regulates endosome morphology and traffic to the degradative pathway through its interaction with Rab4 and c-Cbl. Traffic 4(2), 97-112.
Filocamo, M., Morrone, A., 2011. Lysosomal storage disorders: molecular basis and laboratory testing. Hum Genomics 5(3), 156-169.

Gowrishankar, S., Yuan, P., Wu, Y., Schrag, M., Paradise, S., Grutzendler, J., De Camilli, P., Ferguson, S.M., 2015. Massive accumulation of luminal protease-deficient axonal lysosomes at Alzheimer's disease amyloid plaques. Proc Natl Acad Sci U S A 112(28), E3699-3708.
Harold, D., Abraham, R., Hollingworth, P., Sims, R., Gerrish, A., Hamshere, M.L., Pahwa, J.S., Moskvina, V., Dowzell, K., Williams, A., Jones, N., Thomas, C., Stretton, A., Morgan, A.R., Lovestone, S., Powell, J., Proitsi, P., Lupton, M.K., Brayne, C., Rubinsztein, D.C., Gill, M., Lawlor, B., Lynch, A., Morgan, K., Brown, K.S., Passmore, P.A., Craig, D., McGuinness, B., Todd, S., Holmes, C., Mann, D., Smith, A.D., Love, S., Kehoe, P.G., Hardy, J., Mead, S., Fox, N., Rossor, M., Collinge, J., Maier, W., Jessen, F., Schurmann, B., Heun, R., van den Bussche, H., Heuser, I., Kornhuber, J., Wiltfang, J., Dichgans, M., Frolich, L., Hampel, H., Hull, M., Rujescu, D., Goate, A.M., Kauwe, J.S., Cruchaga, C., Nowotny, P., Morris, J.C., Mayo, K., Sleegers, K., Bettens, K., Engelborghs, S., De Deyn, P.P., Van Broeckhoven, C., Livingston, G., Bass, N.J., Gurling, H., McQuillin, A., Gwilliam, R., Deloukas, P., Al-Chalabi, A., Shaw, C.E., Tsolaki, M., Singleton, A.B., Guerreiro, R., Muhleisen, T.W., Nothen, M.M., Moebus, S., Jockel, K.H., Klopp, N., Wichmann, H.E., Carrasquillo, M.M., Pankratz, V.S., Younkin, S.G., Holmans, P.A., O'Donovan, M., Owen, M.J., Williams, J., 2009. Genome-wide association study identifies variants at CLU and PICALM associated with Alzheimer's disease. Nat Genet 41(10), 1088-1093.
Harris, S.A., Harris, E.A., 2015. Herpes Simplex Virus Type 1 and Other Pathogens are Key Causative Factors in Sporadic Alzheimer's Disease. J Alzheimers Dis 48(2), 319-353.
Hawkes, C., Kabogo, D., Amritraj, A., Kar, S., 2006. Up-regulation of cation-independent mannose 6-phosphate receptor and endosomal-lysosomal markers in surviving neurons after 192-IgG-saporin administrations into the adult rat brain. Am J Pathol 169(4), 1140-1154.
Itzhaki, R.F., Lathe, R., Balin, B.J., Ball, M.J., Bearer, E.L., Braak, H., Bullido, M.J., Carter, C., Clerici, M., Cosby, S.L., Del Tredici, K., Field, H., Fulop, T., Grassi, C., Griffin, W.S., Haas, J., Hudson, A.P., Kamer, A.R., Kell, D.B., Licastro, F., Letenneur, L., Lovheim, H., Mancuso, R., Miklossy, J., Otth, C., Palamara, A.T., Perry, G., Preston, C., Pretorius, E., Strandberg, T., Tabet, N., Taylor-Robinson, S.D., Whittum-Hudson, J.A., 2016. Microbes and Alzheimer's Disease. J Alzheimers Dis 51(4), 979-984.
Itzhaki, R.F., Lin, W.R., Shang, D., Wilcock, G.K., Faragher, B., Jamieson, G.A., 1997. Herpes simplex virus type 1 in brain and risk of Alzheimer's disease. Lancet 349(9047), 241-244.
Johansson, A.C., Appelqvist, H., Nilsson, C., Kagedal, K., Roberg, K., Ollinger, K., 2010. Regulation of apoptosis-associated lysosomal membrane permeabilization. Apoptosis 15(5), 527-540.
Jones, L., Harold, D., Williams, J., 2010. Genetic evidence for the involvement of lipid metabolism in Alzheimer's disease. Biochim Biophys Acta 1801(8), 754-761.
Kim, G.H., Kim, J.E., Rhie, S.J., Yoon, S., 2015. The Role of Oxidative Stress in Neurodegenerative Diseases. Exp Neurobiol 24(4), 325-340.
Koike, M., Nakanishi, H., Saftig, P., Ezaki, J., Isahara, K., Ohsawa, Y., Schulz-Schaeffer, W., Watanabe, T., Waguri, S., Kametaka, S., Shibata, M., Yamamoto, K., Kominami, E., Peters, C., von Figura, K., Uchiyama, Y., 2000. Cathepsin D deficiency induces lysosomal storage with ceroid lipofuscin in mouse CNS neurons. J Neurosci 20(18), 6898-6906.
Laketa, V., Zarbakhsh, S., Traynor-Kaplan, A., Macnamara, A., Subramanian, D., Putyrski, M., Mueller, R., Nadler, A., Mentel, M., Saez-Rodriguez, J., Pepperkok, R., Schultz, C., 2014. PIP(3) induces the recycling of receptor tyrosine kinases. Sci Signal 7(308), ra5.
Lambert, J.C., Heath, S., Even, G., Campion, D., Sleegers, K., Hiltunen, M., Combarros, O., Zelenika, D., Bullido, M.J., Tavernier, B., Letenneur, L., Bettens, K., Berr, C., Pasquier, F., Fievet, N., Barberger-Gateau, P., Engelborghs, S., De Deyn, P., Mateo, I., Franck, A., Helisalmi, S., Porcellini, E., Hanon, O., European Alzheimer's Disease Initiative, I., de Pancorbo, M.M., Lendon, C., Dufouil, C., Jaillard, C., Leveillard, T., Alvarez, V., Bosco, P., Mancuso, M., Panza, F., Nacmias, B., Bossu, P., Piccardi, P., Annoni, G., Seripa, D., Galimberti, D., Hannequin, D., Licastro, F., Soininen, H., Ritchie, K., Blanche, H., Dartigues, J.F., Tzourio, C., Gut, I., Van Broeckhoven, C., Alperovitch, A., Lathrop, M., Amouyel, P., 2009. Genome-wide association

study identifies variants at CLU and CR1 associated with Alzheimer's disease. Nat Genet 41(10), 1094-1099.
Lambert, J.C., Ibrahim-Verbaas, C.A., Harold, D., Naj, A.C., Sims, R., Bellenguez, C., DeStafano, A.L., Bis, J.C., Beecham, G.W., Grenier-Boley, B., Russo, G., Thorton-Wells, T.A., Jones, N., Smith, A.V., Chouraki, V., Thomas, C., Ikram, M.A., Zelenika, D., Vardarajan, B.N., Kamatani, Y., Lin, C.F., Gerrish, A., Schmidt, H., Kunkle, B., Dunstan, M.L., Ruiz, A., Bihoreau, M.T., Choi, S.H., Reitz, C., Pasquier, F., Cruchaga, C., Craig, D., Amin, N., Berr, C., Lopez, O.L., De Jager, P.L., Deramecourt, V., Johnston, J.A., Evans, D., Lovestone, S., Letenneur, L., Moron, F.J., Rubinsztein, D.C., Eiriksdottir, G., Sleegers, K., Goate, A.M., Fievet, N., Huentelman, M.W., Gill, M., Brown, K., Kamboh, M.I., Keller, L., Barberger-Gateau, P., McGuiness, B., Larson, E.B., Green, R., Myers, A.J., Dufouil, C., Todd, S., Wallon, D., Love, S., Rogaeva, E., Gallacher, J., St George-Hyslop, P., Clarimon, J., Lleo, A., Bayer, A., Tsuang, D.W., Yu, L., Tsolaki, M., Bossu, P., Spalletta, G., Proitsi, P., Collinge, J., Sorbi, S., Sanchez-Garcia, F., Fox, N.C., Hardy, J., Deniz Naranjo, M.C., Bosco, P., Clarke, R., Brayne, C., Galimberti, D., Mancuso, M., Matthews, F., European Alzheimer's Disease, I., Genetic, Environmental Risk in Alzheimer's, D., Alzheimer's Disease Genetic, C., Cohorts for, H., Aging Research in Genomic, E., Moebus, S., Mecocci, P., Del Zompo, M., Maier, W., Hampel, H., Pilotto, A., Bullido, M., Panza, F., Caffarra, P., Nacmias, B., Gilbert, J.R., Mayhaus, M., Lannefelt, L., Hakonarson, H., Pichler, S., Carrasquillo, M.M., Ingelsson, M., Beekly, D., Alvarez, V., Zou, F., Valladares, O., Younkin, S.G., Coto, E., Hamilton-Nelson, K.L., Gu, W., Razquin, C., Pastor, P., Mateo, I., Owen, M.J., Faber, K.M., Jonsson, P.V., Combarros, O., O'Donovan, M.C., Cantwell, L.B., Soininen, H., Blacker, D., Mead, S., Mosley, T.H., Jr., Bennett, D.A., Harris, T.B., Fratiglioni, L., Holmes, C., de Bruijn, R.F., Passmore, P., Montine, T.J., Bettens, K., Rotter, J.I., Brice, A., Morgan, K., Foroud, T.M., Kukull, W.A., Hannequin, D., Powell, J.F., Nalls, M.A., Ritchie, K., Lunetta, K.L., Kauwe, J.S., Boerwinkle, E., Riemenschneider, M., Boada, M., Hiltuenen, M., Martin, E.R., Schmidt, R., Rujescu, D., Wang, L.S., Dartigues, J.F., Mayeux, R., Tzourio, C., Hofman, A., Nothen, M.M., Graff, C., Psaty, B.M., Jones, L., Haines, J.L., Holmans, P.A., Lathrop, M., Pericak-Vance, M.A., Launer, L.J., Farrer, L.A., van Duijn, C.M., Van Broeckhoven, C., Moskvina, V., Seshadri, S., Williams, J., Schellenberg, G.D., Amouyel, P., 2013. Meta-analysis of 74,046 individuals identifies 11 new susceptibility loci for Alzheimer's disease. Nat Genet 45(12), 1452-1458.
Leow, S.M., Chua, S.X., Venkatachalam, G., Shen, L., Luo, L., Clement, M.V., 2017. Sub-lethal oxidative stress induces lysosome biogenesis via a lysosomal membrane permeabilization-cathepsin-caspase 3-transcription factor EB-dependent pathway. Oncotarget 8(10), 16170-16189.
Lerchundi, R., Neira, R., Valdivia, S., Vio, K., Concha, M.I., Zambrano, A., Otth, C., 2011. Tau cleavage at D421 by caspase-3 is induced in neurons and astrocytes infected with herpes simplex virus type 1. J Alzheimers Dis 23(3), 513-520.
Letenneur, L., Peres, K., Fleury, H., Garrigue, I., Barberger-Gateau, P., Helmer, C., Orgogozo, J.M., Gauthier, S., Dartigues, J.F., 2008. Seropositivity to herpes simplex virus antibodies and risk of Alzheimer's disease: a population-based cohort study. PLoS One 3(11), e3637.
Licastro, F., Carbone, I., Ianni, M., Porcellini, E., 2011. Gene signature in Alzheimer's disease and environmental factors: the virus chronicle. J Alzheimers Dis 27(4), 809-817.
Lovheim, H., Gilthorpe, J., Adolfsson, R., Nilsson, L.G., Elgh, F., 2015a. Reactivated herpes simplex infection increases the risk of Alzheimer's disease. Alzheimers Dement 11(6), 593-599.
Lovheim, H., Gilthorpe, J., Johansson, A., Eriksson, S., Hallmans, G., Elgh, F., 2015b. Herpes simplex infection and the risk of Alzheimer's disease: A nested case-control study. Alzheimers Dement 11(6), 587-592.
Mancuso, R., Baglio, F., Cabinio, M., Calabrese, E., Hernis, A., Nemni, R., Clerici, M., 2014. Titers of herpes simplex virus type 1 antibodies positively correlate with grey matter volumes in Alzheimer's disease. J Alzheimers Dis 38(4), 741-745.

Martin, C., Aguila, B., Araya, P., Vio, K., Valdivia, S., Zambrano, A., Concha, M.I., Otth, C., 2014. Inflammatory and neurodegeneration markers during asymptomatic HSV-1 reactivation. J Alzheimers Dis 39(4), 849-859.
Moreau, K., Fleming, A., Imarisio, S., Lopez Ramirez, A., Mercer, J.L., Jimenez-Sanchez, M., Bento, C.F., Puri, C., Zavodszky, E., Siddiqi, F., Lavau, C.P., Betton, M., O'Kane, C.J., Wechsler, D.S., Rubinsztein, D.C., 2014. PICALM modulates autophagy activity and tau accumulation. Nat Commun 5, 4998.
Neefjes, J., van der Kant, R., 2014. Stuck in traffic: an emerging theme in diseases of the nervous system. Trends Neurosci 37(2), 66-76.
Niazy, N., Temme, S., Bocuk, D., Giesen, C., Konig, A., Temme, N., Ziegfeld, A., Gregers, T.F., Bakke, O., Lang, T., Eis-Hubinger, A.M., Koch, N., 2017. Misdirection of endosomal trafficking mediated by herpes simplex virus-encoded glycoprotein B. FASEB J 31(4), 1650-1667.
Nixon, R.A., Yang, D.S., Lee, J.H., 2008. Neurodegenerative lysosomal disorders: a continuum from development to late age. Autophagy 4(5), 590-599.
Nogales-Cadenas, R., Carmona-Saez, P., Vazquez, M., Vicente, C., Yang, X., Tirado, F., Carazo, J.M., Pascual-Montano, A., 2009. GeneCodis: interpreting gene lists through enrichment analysis and integration of diverse biological information. Nucleic Acids Res 37(Web Server issue), W317-322.
Peric, A., Annaert, W., 2015. Early etiology of Alzheimer's disease: tipping the balance toward autophagy or endosomal dysfunction? Acta Neuropathol 129(3), 363-381.
Piacentini, R., De Chiara, G., Li Puma, D.D., Ripoli, C., Marcocci, M.E., Garaci, E., Palamara, A.T., Grassi, C., 2014. HSV-1 and Alzheimer's disease: more than a hypothesis. Front Pharmacol 5, 97.
Piacentini, R., Li Puma, D.D., Ripoli, C., Marcocci, M.E., De Chiara, G., Garaci, E., Palamara, A.T., Grassi, C., 2015. Herpes Simplex Virus type-1 infection induces synaptic dysfunction in cultured cortical neurons via GSK-3 activation and intraneuronal amyloid-beta protein accumulation. Sci Rep 5, 15444.
Polito, V.A., Li, H., Martini-Stoica, H., Wang, B., Yang, L., Xu, Y., Swartzlander, D.B., Palmieri, M., di Ronza, A., Lee, V.M., Sardiello, M., Ballabio, A., Zheng, H., 2014. Selective clearance of aberrant tau proteins and rescue of neurotoxicity by transcription factor EB. EMBO Mol Med 6(9), 1142-1160.
Porcellini, E., Carbone, I., Ianni, M., Licastro, F., 2010. Alzheimer's disease gene signature says: beware of brain viral infections. Immun Ageing 7, 16.
Porter, K., Nallathambi, J., Lin, Y., Liton, P.B., 2013. Lysosomal basification and decreased autophagic flux in oxidatively stressed trabecular meshwork cells: Implications for glaucoma pathogenesis. Autophagy 9(4), 581-594.
Recuero, M., Munive, V.A., Sastre, I., Aldudo, J., Valdivieso, F., Bullido, M.J., 2013. A free radical-generating system regulates AbetaPP metabolism/processing: involvement of the ubiquitin/proteasome and autophagy/lysosome pathways. J Alzheimers Dis 34(3), 637-647.
Recuero, M., Munoz, T., Aldudo, J., Subias, M., Bullido, M.J., Valdivieso, F., 2010. A free radical-generating system regulates APP metabolism/processing. FEBS Lett 584(22), 4611-4618.
Recuero, M., Vicente, M.C., Martinez-Garcia, A., Ramos, M.C., Carmona-Saez, P., Sastre, I., Aldudo, J., Vilella, E., Frank, A., Bullido, M.J., Valdivieso, F., 2009. A free radical-generating system induces the cholesterol biosynthesis pathway: a role in Alzheimer's disease. Aging Cell 8(2), 128-139.
Santana, S., Bullido, M.J., Recuero, M., Valdivieso, F., Aldudo, J., 2012a. Herpes simplex virus type I induces an incomplete autophagic response in human neuroblastoma cells. J Alzheimers Dis 30(4), 815-831.
Santana, S., Recuero, M., Bullido, M.J., Valdivieso, F., Aldudo, J., 2012b. Herpes simplex virus type I induces the accumulation of intracellular beta-amyloid in autophagic compartments and the inhibition of the non-amyloidogenic pathway in human neuroblastoma cells. Neurobiol Aging 33(2), 430 e419-433.

Santana, S., Sastre, I., Recuero, M., Bullido, M.J., Aldudo, J., 2013. Oxidative stress enhances neurodegeneration markers induced by herpes simplex virus type 1 infection in human neuroblastoma cells. PLoS One 8(10), e75842.
Smyth, G.K., 2004. Linear models and empirical bayes methods for assessing differential expression in microarray experiments. Stat Appl Genet Mol Biol 3, Article3.
Sun, B., Zhou, Y., Halabisky, B., Lo, I., Cho, S.H., Mueller-Steiner, S., Devidze, N., Wang, X., Grubb, A., Gan, L., 2008. Cystatin C-cathepsin B axis regulates amyloid beta levels and associated neuronal deficits in an animal model of Alzheimer's disease. Neuron 60(2), 247-257.
Tabas-Madrid, D., Nogales-Cadenas, R., Pascual-Montano, A., 2012. GeneCodis3: a non-redundant and modular enrichment analysis tool for functional genomics. Nucleic Acids Res.
Tang, C.H., Lee, J.W., Galvez, M.G., Robillard, L., Mole, S.E., Chapman, H.A., 2006. Murine cathepsin F deficiency causes neuronal lipofuscinosis and late-onset neurological disease. Mol Cell Biol 26(6), 2309-2316.
Turk, V., Turk, B., Turk, D., 2001. Lysosomal cysteine proteases: facts and opportunities. EMBO J 20(17), 4629-4633.
van Weering, D.H., Medema, J.P., van Puijenbroek, A., Burgering, B.M., Baas, P.D., Bos, J.L., 1995. Ret receptor tyrosine kinase activates extracellular signal-regulated kinase 2 in SK-N-MC cells. Oncogene 11(11), 2207-2214.
Whyte, L.S., Lau, A.A., Hemsley, K.M., Hopwood, J.J., Sargeant, T.J., 2017. Endo-lysosomal and autophagic dysfunction: a driving factor in Alzheimer's disease? J Neurochem 140(5), 703-717.
Wolfe, D.M., Lee, J.H., Kumar, A., Lee, S., Orenstein, S.J., Nixon, R.A., 2013. Autophagy failure in Alzheimer's disease and the role of defective lysosomal acidification. Eur J Neurosci 37(12), 1949-1961.
Wozniak, M.A., Frost, A.L., Itzhaki, R.F., 2013. The helicase-primase inhibitor BAY 57-1293 reduces the Alzheimer's disease-related molecules induced by herpes simplex virus type 1. Antiviral Res 99(3), 401-404.
Wozniak, M.A., Frost, A.L., Preston, C.M., Itzhaki, R.F., 2011. Antivirals reduce the formation of key Alzheimer's disease molecules in cell cultures acutely infected with herpes simplex virus type 1. PLoS One 6(10), e25152.
Wozniak, M.A., Itzhaki, R.F., Shipley, S.J., Dobson, C.B., 2007. Herpes simplex virus infection causes cellular beta-amyloid accumulation and secretase upregulation. Neurosci Lett 429(2-3), 95-100.
Wozniak, M.A., Mee, A.P., Itzhaki, R.F., 2009. Herpes simplex virus type 1 DNA is located within Alzheimer's disease amyloid plaques. J Pathol 217(1), 131-138.
Xiao, Q., Yan, P., Ma, X., Liu, H., Perez, R., Zhu, A., Gonzales, E., Tripoli, D.L., Czerniewski, L., Ballabio, A., Cirrito, J.R., Diwan, A., Lee, J.M., 2015. Neuronal-Targeted TFEB Accelerates Lysosomal Degradation of APP, Reducing Abeta Generation and Amyloid Plaque Pathogenesis. J Neurosci 35(35), 12137-12151.
Yang, D.S., Stavrides, P., Saito, M., Kumar, A., Rodriguez-Navarro, J.A., Pawlik, M., Huo, C., Walkley, S.U., Saito, M., Cuervo, A.M., Nixon, R.A., 2014. Defective macroautophagic turnover of brain lipids in the TgCRND8 Alzheimer mouse model: prevention by correcting lysosomal proteolytic deficits. Brain 137(Pt 12), 3300-3318.
Zambrano, A., Solis, L., Salvadores, N., Cortes, M., Lerchundi, R., Otth, C., 2008. Neuronal cytoskeletal dynamic modification and neurodegeneration induced by infection with herpes simplex virus type 1. J Alzheimers Dis 14(3), 259-269.

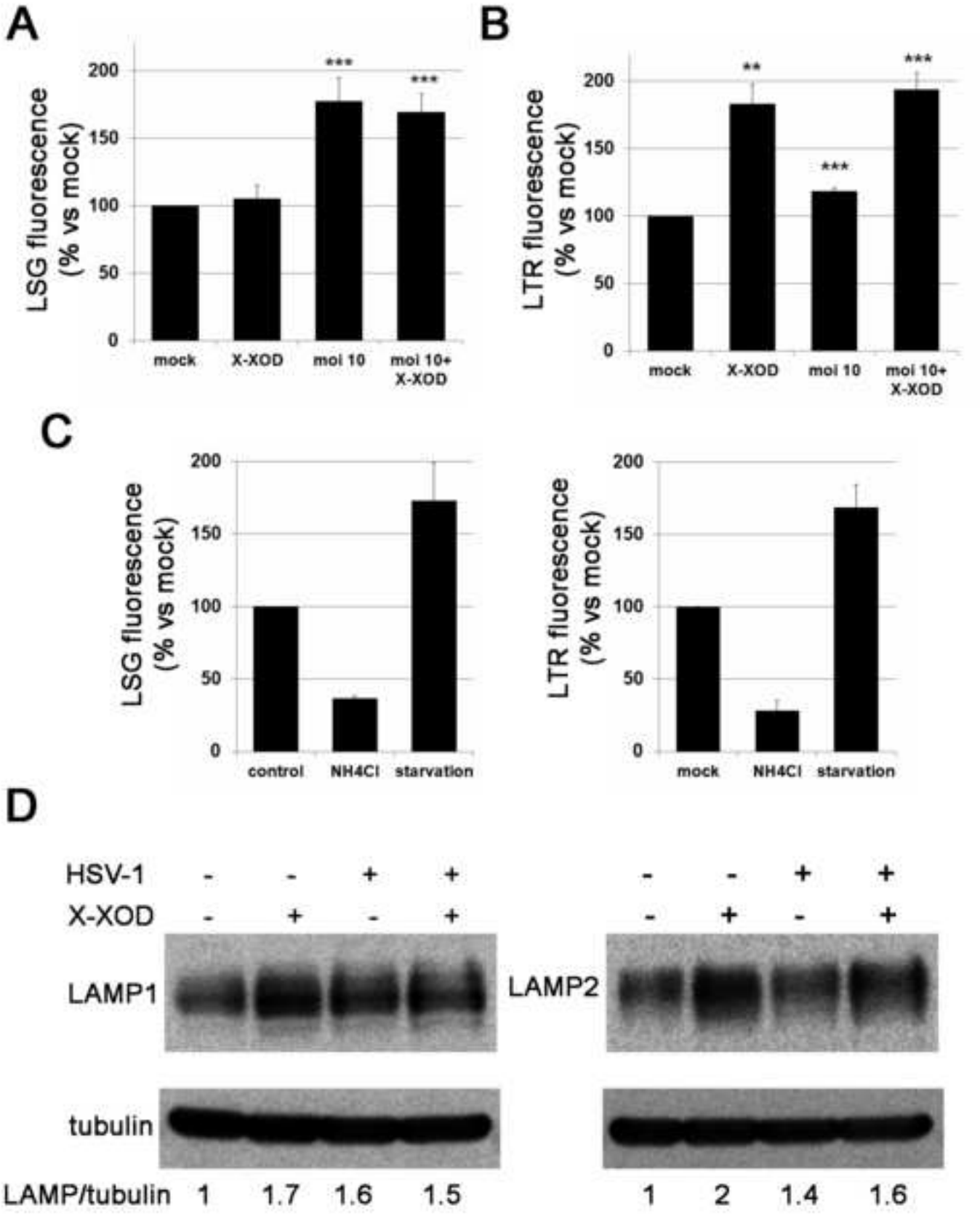
A
LSG fluorescence (% vs mock)
200
150
100
50
0
***
***
mock
X-XOD
moi 10
moi 10+ X-XOD
B
LTR fluorescence (% vs mock)
200
150
100
50
0
**
***
***
mock
X-XOD
moi 10
moi 10+ X-XOD
C
LSG fluorescence (% vs mock)
200
150
100
50
0
control
NH4Cl
starvation
LTR fluorescence (% vs mock)
200
150
100
50
0
mock
NH4Cl
starvation
D
HSV-1 - - + +
X-XOD - + - +
LAMP1
tubulin
LAMP/tubulin 1 1.7 1.6 1.5
HSV-1 - - + +
X-XOD - + - +
LAMP2
1 2 1.4 1.6

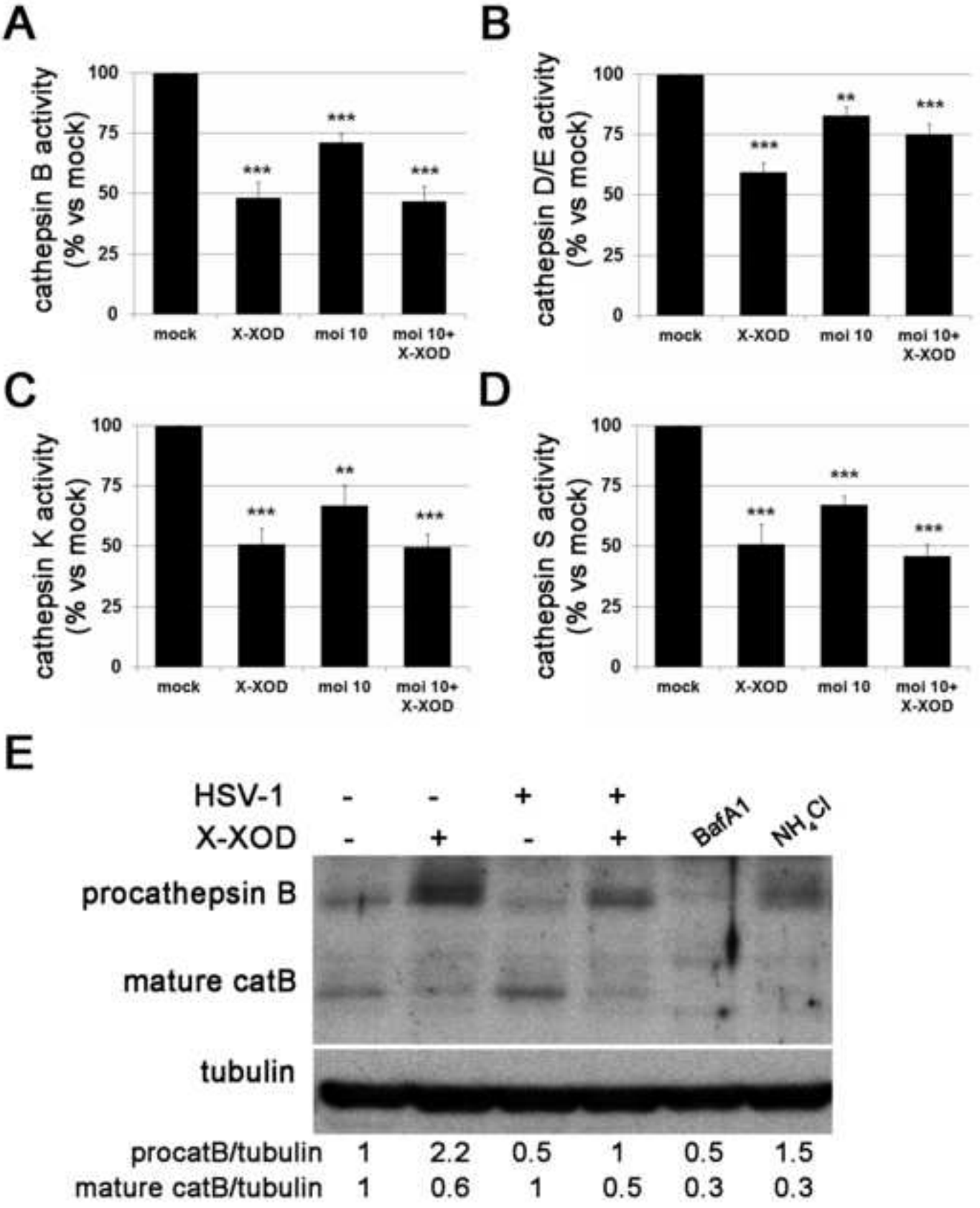
A
cathepsin B activity (% vs mock)
100
75
50
25
0
***
***
***
mock
X-XOD
moi 10
moi 10+ X-XOD
B
cathepsin D/E activity (% vs mock)
***
**
***
C
cathepsin K activity (% vs mock)
***
**
***
D
cathepsin S activity (% vs mock)
***
***
***
E
HSV-1 - - + +
X-XOD - + - +
BafA1
NH4Cl
procathepsin B
mature catB
tubulin
procatB/tubulin 1 2.2 0.5 1 0.5 1.5
mature catB/tubulin 1 0.6 1 0.5 0.3 0.3

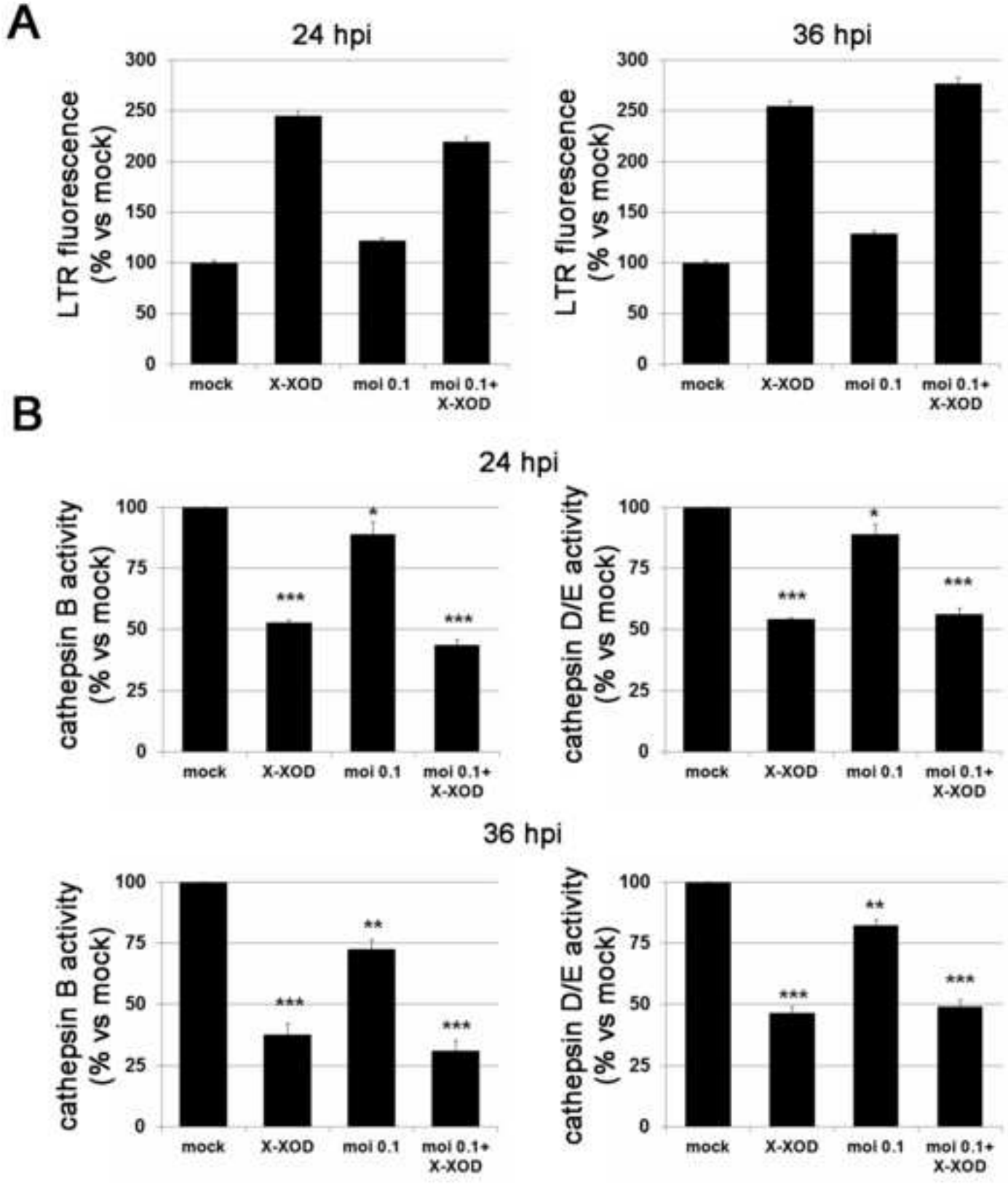
A
24 hpi
36 hpi
LTR fluorescence (% vs mock)
300
250
200
150
100
50
0
mock
X-XOD
moi 0.1
moi 0.1+ X-XOD
B
24 hpi
cathepsin B activity (% vs mock)
cathepsin D/E activity (% vs mock)
100
75
50
25
0
*
**
***
36 hpi

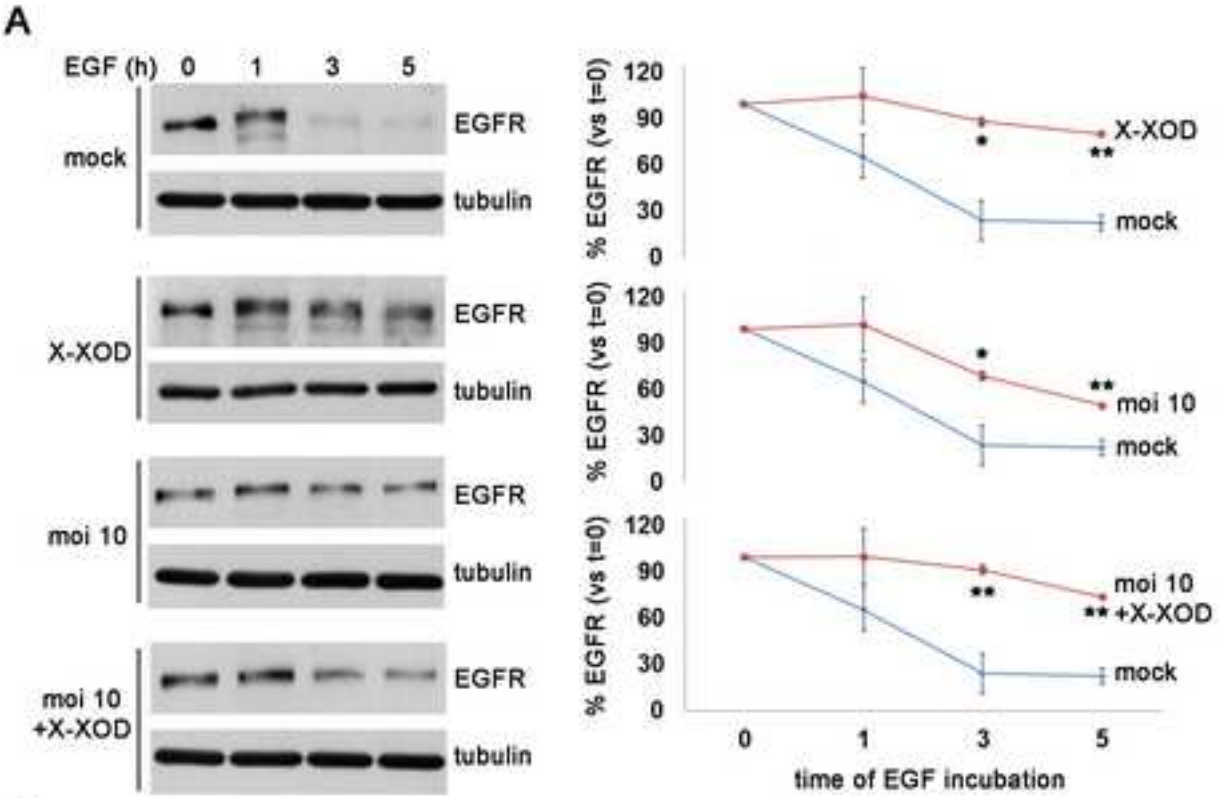

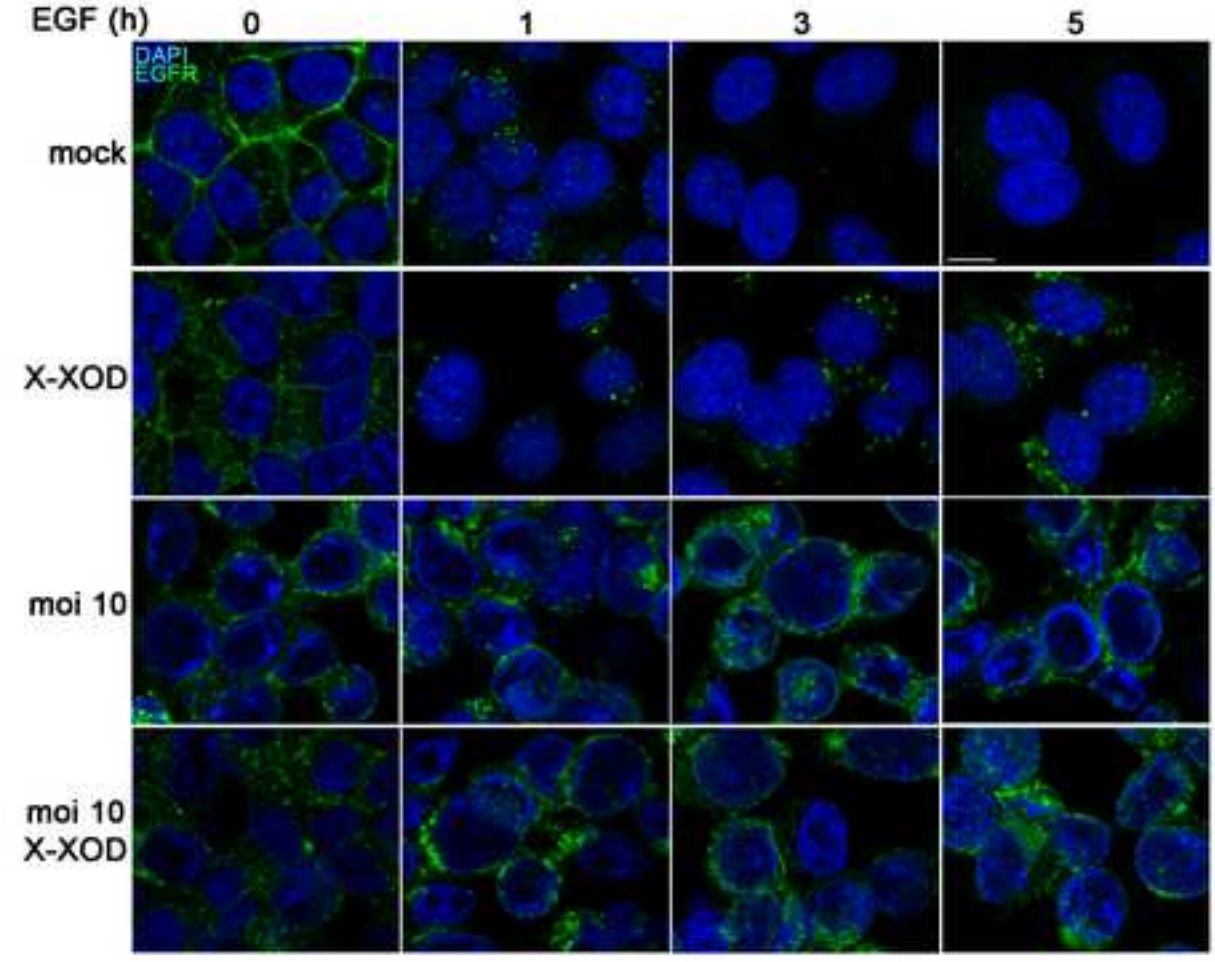

Color in print

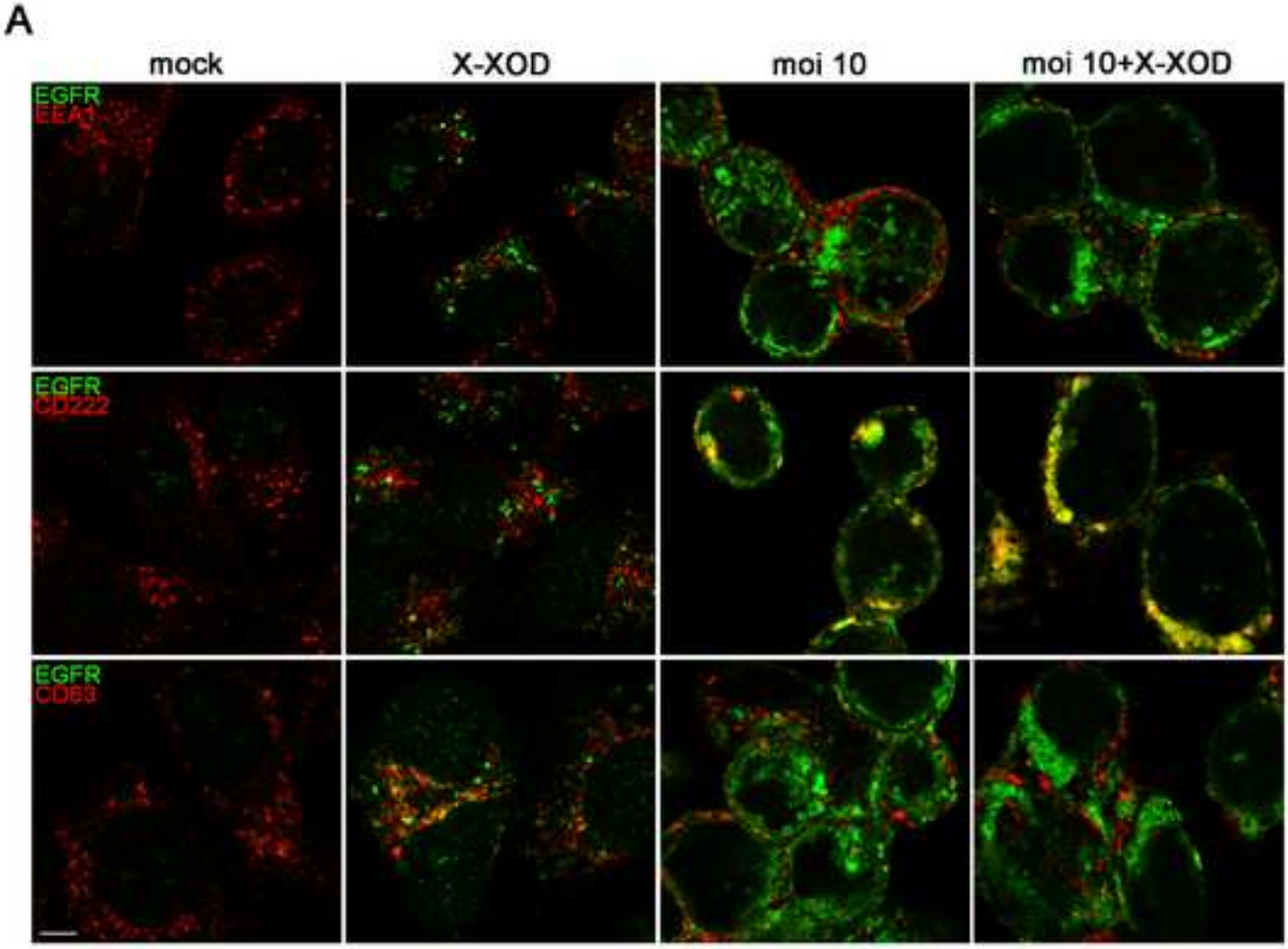

Color in print

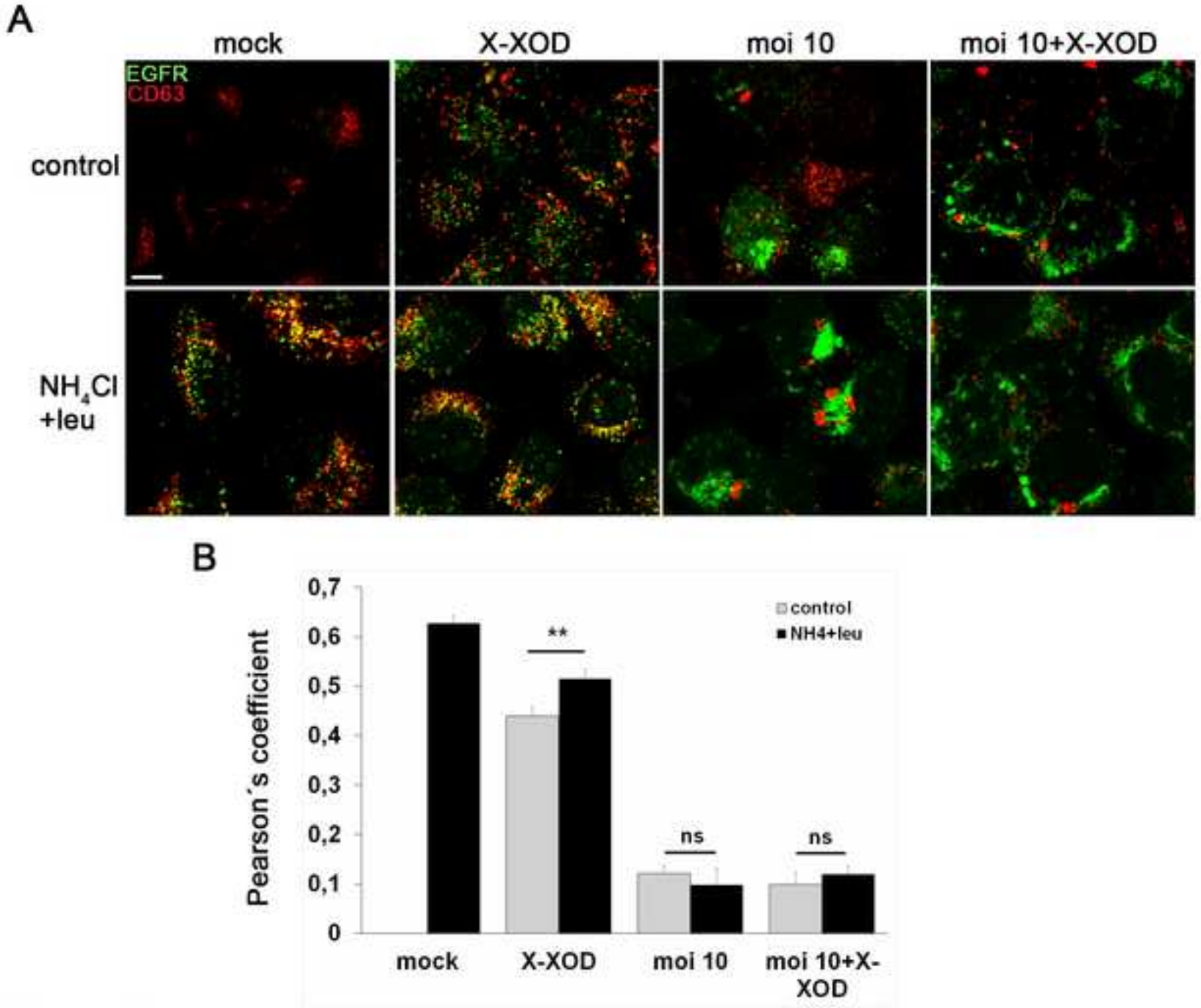

Color in print

FIGURE CAPTIONS

Figure 1. Effect of OS and HSV-1 infection on lysosome load. After HSV-1 infection (moi 10) and X-XOD, NH_4Cl and starvation treatments, SK-N-MC cells were loaded with either LysoSensor Green (LSG) or LysoTracker Red (LTR) for 1 h. **(A)** LSG fluorescence was quantified by flow cytometry in the green spectrum (FL-1 channel). **(B)** LTR fluorescence was recorded using a microplate reader. **(C)** As a control, cells were exposed to NH_4Cl and nutrient starvation. In **(A)** and **(B),** graphs represent the mean ± SEM of five experiments, and in **(C)** the mean ± SD of two experiments. Data are expressed as the percentage with respect to non-infected cells (mock) (**p<0.01, ***p<0.001). **D)** SK-N-MC cells were treated with X-XOD and infected with HSV-1 at a moi of 10 pfu/cell for 18 h and Western blot analysis with anti-LAMP1, anti-LAMP2 and anti-tubulin antibodies were performed. LAMP1 and LAMP2 levels were determined by densitometric analysis and the ratio of LAMP proteins to tubulin is shown below the blots. Data are the mean of two experiments.

Figure 2. HSV-1 and OS induce a reduction of lysosomal enzyme activity. SK-N-MC cells were exposed to HSV-1 (moi 10) and X-XOD for 18 h. The relative enzymatic activities (compared with mock-infected cells) of cathepsins B **(A)**, D and E **(B)**, K **(C)** and S **(D)** were quantified and normalized by the protein content of the lysates. Data are the mean ± SEM of at least four experiments (**p<0.01, ***p<0.001). **E)** SK-N-MC cells were exposed to HSV-1 (moi 10) and X-XOD or incubated with bafilomycin A1 (BafA1) or ammonium chloride for 18 h and cathepsin B levels were analyzed by Western blot. A tubulin blot is shown as a control for equal loading. Procathepsin and mature cathepsin B amount was determined by densitometric analysis and the ratio of cathepsin B to tubulin is shown below the blots. Data are the mean of two experiments.

Figure 3. Effect of lower doses of HSV-1 on lysosomal content and cathepsin activities. SK-N-MC cells were treated with X-XOD and infected with HSV-1 at a moi of 0.1 pfu/cell for 24 or 36 h. **A)** LysoTracker Red (LTR) fluorescence was quantified using a microplate reader. Graphs represent the mean ± SD of a representative experiment performed in triplicate; data are expressed as a percentage with respect to mock-infected cells. **B)** The relative enzymatic activities, compared with mock-infected cells, of cathepsins B and D/E were quantified and normalized by the protein content of the lysates. Data are the mean ± SEM of three experiments (*p<0.05, **p<0.01, ***p<0.001).

Figure 4. HSV-1 and OS impair lysosomal degradation of EGFR. HeLa cells were treated with HSV-1 (moi 10) and X-XOD for 13 h and EGFR degradation then determined by stimulating the cells with 40 ng/ml EGF for the indicated times to induce EGFR internalization. **A)** Western blot analysis was performed with anti-EGFR and anti-tubulin antibodies. EGFR degradation was determined by quantifying the amount of remaining EGFR via densitometric analysis and normalized against tubulin. Graphical data represent the mean ± SEM of three experiments and are expressed as the percentage quantity of EGFR present at time t=0 (100%) (*p<0.05, **p<0.01). **B)** Immunofluorescence images of HeLa cells using an anti-EGFR antibody. DAPI-stained nuclei are shown. DAPI staining reveals HSV-1 to induce the generation of black patches corresponding to chromatin margination. Note the accumulation of EGFR in cells exposed to OS and HSV-1. Scale bar: 10 µm.

Figure 5. Internalized EGFR colocalizes with late endosomal markers in HSV-1-infected cells. **A)** HeLa cells were exposed to HSV-1 (moi 10) and X-XOD for 18 h. 5 h before the end of treatments, HeLa cells were stimulated with 40 ng/ml EGF and the

colocalization of EGFR with early endosomal (EEA1), late endosomal (CD222), and lysosomal (CD63) markers analyzed by confocal microscopy. The yellow color in the merged panels indicates colocalization of signals. Scale bar: 5 µm. **B)** Quantification of the colocalization of EGFR and endolysosomal markers. Confocal fluorescence images were analyzed as described in Materials and Methods. The graph shows the relative colocalization (Pearson´s correlation coefficient). Significance was determined using a Student t-test (***p<0.001).

Figure 6. Colocalization analysis of EGFR with lysosomal markers in the presence of lysosomal inhibitors. A) HeLa cells were treated with X-XOD and infected with HSV-1 at a moi of 10 pfu/cell for 18 h in the absence or presence of the lysosomal inhibitors leupeptin (leu) and ammonium chloride (NH4Cl). 5 h before the end of treatments, HeLa cells were stimulated with 40 ng/ml EGF and the colocalization of EGFR with the lysosomal marker CD63 analyzed by confocal microscopy. The yellow color in the merged panels indicates colocalization of signals. Scale bar: 5 µm. **B)** Quantification of the colocalization of EGFR and CD63 stainings. Confocal fluorescence images were analyzed as described in Materials and Methods. The graph shows the relative colocalization (Pearson´s correlation coefficient). Significance was determined using a Student t-test (**p<0.01; ns: non-significant).